IR 81-2252 R

MHD MATERIALS - SEED/SLAG INTERACTIONS AND EFFECTS

QUARTERLY PROGRESS REPORT

October 1 - December 31, 1980

Samuel J. Schneider
Project Manager

Center for Materials Science
U. S. Department of Commerce
National Bureau of Standards
Washington, D. C. 20234

PREPARED FOR THE UNITED STATES
DEPARTMENT OF ENERGY
MHD OFFICE

"This report was prepared as an account of work sponsored by the United States Government. Neither the United States nor the United States Department of Energy, nor any of their employees, nor any of their contractors, subcontractors, or their employees, makes any warranty, express or implied, or assumes any legal liability or responsibility for the accuracy, completeness, or usefulness of any information, apparatus, product or process disclosed, or represents that its use would not infringe privately owned rights."

TABLE OF CONTENTS

		Page
I.	SUMMARY OF PROGRESS TO DATE.	1
II.	DETAILED DESCRIPTION OF TECHNICAL PROGRESS	2
	1. Thermochemistry of Seed and Slag.	2
	2. Electrical Conductivity and Polarization.	11
	3. Corrosion of Downstream MHD Components.	18

I. SUMMARY OF PROGRESS TO DATE

1. Thermochemistry of Seed and Slag

New K pressure data on a Western-type slag initially containing 20 wt% K_2O are presented. The decrease in K pressure with decreasing K_2O composition is less than in previous measurements. Analysis of previous data shows a decrease in K pressure of 20 percent for unit decrease in wt% K_2O and an increase in K pressure of 8 percent for unit increase in wt% CaO.

A series of 3 types of experiments for conclusive test of subsolidus equilibria involving 12 compounds in the system K_2O-CaO-Al_2O_3-SiO_2 has been devised and is nearly complete. Initial indications are that the previously postulated equilibrium diagram is essentially correct. However, an important modification must be made to allow for the presence of potassium-deficient $KAlSi_2O_6$ (ss). Existence of this previously unreported solid solution may have significant effect on the thermodynamics of K_2O vaporization or absorption involving this phase.

2. Electrical Conductivity and Polarization

Both AC and DC conductivity measurements have been initiated on a Western slag derived from coal from the Rosebud seam in Montana. These measurements are designed to investigate the conductivity mechanism in this slag which contains a minimal amount of iron (approximately 4 w/o) compared to a typical Eastern slag (approximately 12-16%). In this report, primary emphasis is placed on measurements in the temperature range between 1200 and 1500 °C.

Measurements were made on a sample of yttria stabilized zirconia in an effort to verify the measurement technique on a purely ionic conductor of a given single phase composition.

3. Corrosion of Downstream MHD Components

Optical and SEM and EDX analysis were undertaken on sections of Type 316 stainless steel tubing exposed to fuel rich and oxygen rich hot gas streams seeded with 80% by weight K_2CO_3 and 20% by weight K_2SO_4. Analysis revealed only slight differences as a result of the hot gas stream state. Distribution of species, Fe, Ni and Cr in the reaction zone, (stainless steel - deposit interface) paralleled observations made on Type 304 stainless steel and detailed in previous reports.

II. DETAILED DESCRIPTION OF TECHNICAL PROGRESS

1. Thermochemistry of Seed and Slag (E. R. Plante and L. P. Cook)

A. Vaporization Studies (E. R. Plante)

Progress: Vapor pressure measurements were continued on selected compositions in the K_2O-CaO-Al_2O_3-SiO_2 system. As in prior work, vapor pressures were determined using a Knudsen-effusion, modulated beam mass spectrometric method.

Previous measurements have shown within the limited composition ranges studied that the K_2O activity as determined from measurements of the K and O_2 pressures is insensitive to the individual Al_2O_3 and SiO_2 concentrations, but is decreased as the sum of the Al_2O_3 and SiO_2 concentrations is increased, increased by an increasing CaO concentration and increased by an increasing K_2O concentration.

One of the objectives of the current research is to attempt to construct a simplified model to predict interaction of seeded MHD combustion gases with Western-type coal ash. Thus far, measurements have been completed on three compositions and are in progress on a fourth composition. Table 1 lists the sample designation, starting mineral constituents and wt% of each of the four components for the compositions being studied, as well as the final concentration of components.

The composition of KCAS-VP-4 was selected in order to increase the range of K_2O concentrations studied. There is evidence from engineering studies on seeded MHD combustion products that K_2O absorption by Western-type slags might lead to a final K_2O concentration of as much as 20 wt% K_2O. The composition for KCAS-VP-4 listed in Table 1 was arrived at by neglecting the minor components in a Rosebud ash analysis and replacing the MgO and Fe_2O_3 components with the same amounts of CaO and Al_2O_3 respectively on a wt basis. The composition data for the Rosebud ash and synthetic ash composition are shown in Table 2. This composition was closely approximated using a mixture of the minerals, 66.9 wt% $KAlSiO_4$ and 33.1 wt% Ca_2SiO_4.

Some data selected from the KCAS-VP-4 experiment are shown in figure 1 and compared with a line representing data obtained from the KCAS-VP-1 data in the 14.8-12.4 wt% composition range. Qualitatively, the agreement is satisfactory but the decrease in K pressure with K_2O composition is not as great as was observed in the KCAS-VP-1 experiments. Thus, K pressures shown with a K_2O concentration in the 7-10 wt% range are about a factor of 2 greater than those from the KCAS-VP-1 experiment when the condensed phase contains 14.8-12.4 wt% K_2O. It does not appear likely that this difference is due to variations in the concentrations of the other constituents in the melt because the CaO concentration is actually greater for the KCAS-VP-1 melt by a few percent while the Al_2O_3 and SiO_2 concentrations vary by only a few percent. Thus, there must be

other differences in the experimental measurements responsible for the increase in pressure and its slower decrease in K pressure with decreasing K_2O content. Additional study of this problem is required.

In the previous report, it was noted that measurements in the KCAS-VP-2 and KCAS-VP-3 series appeared to be consistent with each other if the K pressure was dependent at fixed temperature, only on the K_2O and CaO concentration. These data have now been fit to the equation,

$$\log P_K = 3.492 - 16153/T + .0903(\text{wt\% } K_2O) + .0351(\text{wt\% CaO}).$$

The standard deviation in the fit is 30 percent with maximum deviations in individual points of about 100 percent. It is interesting to note that the above equation predicts an increase in K pressure of 20 percent for an increase of 1 wt% K_2O and an increase in K pressure of 8 percent for 1 wt% increase in CaO.

Table 1. Mineral Constituents and Composition of Vaporization Samples

Sample	Mineral Constituents (Wt%)	Initial/Final Composition Wt% K_2O	CaO	Al_2O_3	SiO_2
KCAS-VP-1	$KAlSiO_4$ (49.8), Ca_2SiO_4 (16.5)	14.8	27.5	22.2	35.5
	$Ca_2Al_2SiO_7$ (16.5), $Ca_3Si_2O_7$ (17.2)	1.6	31.8	25.7	40.9
KCAS-VP-2	$KAlSiO_4$ (28.6), $KAlSi_2O_6$ (13.8)	11.5	17.6	33.7	37.2
	$Ca_2Al_2SiO_7$ (28.9), $CaAl_2Si_2O_8$ (28.7)	6.1	18.7	35.7	39.5
KCAS-VP-3	$KAlSiO_4$ (42.0), $CaSiO_3$ (58.0)	12.5	28.0	13.5	46.0
		1.8	31.4	15.2	51.6
KCAS-VP-4	$KAlSiO_4$ (66.9), Ca_2SiO_4 (33.1)	19.9	21.6	21.6	37.0
		7.1	25.0	25.0	42.9

Table 2. Synthetic Composition Approximating Rosebud Ash with 20 wt% K_2O

Component	Rosebud Ash[(a)] Wt%	Simplified Composition	$KAlSiO_4$ (66.9 wt%) Ca_2SiO_4 (33.1 wt%)
SiO_2	40.34	34.32	36.96
Al_2O_3	24.60	24.67	21.56
CaO	18.90	21.02	21.56
MgO	5.80	--	
Fe_2O_3	4.40	--	
K_2O	.53	20.00	19.92
Na_2O	.46	--	
SO_3	.28	--	

(a) R. Pollina and R. Larsen, ANL-77-21 (1977)

B. Phase Equilibrium Studies - The System K_2O-CaO-Al_2O_3-SiO_2 (L. P. Cook)

During the past quarter, experiments have concentrated on finalizing subsolidus equilibrium relations in the (Si, Al)-rich part of the quarternary system. The portion of the system under consideration (Fig. 2) involves 12 crystalline solids and 13 four-phase volumes. As noted in previous quarterly reports, the first melt to appear upon heating each of the four-phase combinations bears a definite relationship to the thermodynamic properties of the solids involved, allowing calculation of an equilibrium P_{K_2O}. Therein lies the basis for construction of a quantitative four-component model for calculation of potassium activities as a function of composition for K_2O-CaO-Al_2O_3-SiO_2 melts simulating Western slags. Such a phase- equilibrium-derived model is useful for supplementing models based on direct measurement of potassium pressures, with the resultant feedback allowing refinement of the thermodynamic properties of the solids. For such a model to be accurate, subsolidus relations must be well known. Unfortunately, 1200-1250 °C appears to be the limit for comprehensive subsolidus studies, and so kinetic factors must be considered in the experimental approach. For this reason, it was thought essential to conclusively verify the results of earlier preliminary work with a new series of experiments. This is being done with three types of experiments, as follows:

1. 1000-Hour Subsolidus Equilibrations

These experiments are being conducted at 1200 °C for 9 of the 13 four-phase volumes and at lower temperatures for the assemblages containing $KAlSi_3O_8$. The procedure is to seal carefully mixed equal weights of the four solids thought to be in equilibrium in Pt capsules, heat them, quench, examine by x-ray, regrind, reseal and reheat. In this way thermodynamically important solid solutions can be detected by subtle shifts in the x-ray parameters. So far no shifts have been detected after 764 hours. However, evidence has been found for potassium-deficient $KAlSi_2O_6$ (ss) showing no change in unit cell parameters (see discussion of second type of experiment below). The 1000-hour equilibrations are $\sim$ 90 percent complete at the time of writing and results will be fully discussed in the next quarterly report. It is hoped that a formal publication describing the results can also be prepared.

2. Solid-State Tie Line Reactions Using Unstable Combinations of Phases

The purpose of these experiments was to verify as many of the tie lines in Fig. 2 as possible by starting with alternative solid assemblages. Reaction to produce the postulated tie line is proof of its relative stability. Eleven tie lines can be investigated in this way as follows (the tie line believed to be stable is on the right):

(1) $11Ca_2SiO_4 + 1KAlSi_2O_6 + 2CaAl_{12}O_{19} \rightarrow 1KAlSiO_4 + 12Ca_2Al_2SiO_7$

(2) $2CaO + 1KAlSi_2O_6 \rightarrow 1KAlSiO_4 + 1Ca_2SiO_4$

(3) $3Ca_2SiO_4 + 1KAlSi_2O_6 \rightarrow 1KAlSiO_4 + 2Ca_3Si_2O_7$

(4) $1Ca_3Si_2O_7 + 1KAlSi_2O_6 \rightarrow 1KAlSiO_4 + 3CaSiO_3$

(5) $3Ca_2Al_2SiO_7 + 1(3Al_2O_3 \cdot 2SiO_2) + 7KAlSi_2O_6 \rightarrow 7KAlSiO_4 + 6CaAl_2Si_2O_8$

(6) $3Ca_2Al_2SiO_7 + 11(3Al_2O_3 \cdot 2SiO_2) + 25KAlO_2 \rightarrow 25KAlSiO_4 + 6CaAl_{12}O_{19}$

(7) $2KAlSiO_4 + 1CaAl_2Si_2O_8 + CaSiO_3 \rightarrow 2KAlSi_2O_6 + 1Ca_2Al_2SiO_7$

(8) $3Ca_2Al_2SiO_7 + 1(3Al_2O_3 \cdot 2SiO_2) + 7KAlSi_3O_8 \rightarrow 7KAlSi_2O_6 + 6CaAl_2Si_2O_8$

(9) $2Ca_3Si_2O_7 + 2KAlSi_3O_8 \rightarrow 2KAlSi_2O_6 + 6CaSiO_3$

(10) $5K_2Si_2O_5 + CaAl_{12}O_{19} + 22SiO_2 \rightarrow 10KAlSi_3O_8 + 1CaAl_2Si_2O_8$

(11) $6K_2Si_2O_5 + 1CaAl_{12}O_{19} + 25SiO_2 \rightarrow 12KAlSi_3O_8 + 1CaSiO_3$

Results of these experiments are summarized in Table 3 below. Tie line reactions 8 and 9 were not investigated because of the current unavailability of $KAlSi_3O_8$ starting materials. Study of tie line reactions 10 and 11 was not successful due to the low-melting nature of these compositions.

Table 3. Tie Line Reactions

Reaction	Starting Materials	Temp. (°C)	Duration (Hr.)	Products
1	γ-C_2S, CA_6, (Lc)	1250 1250	23 64	β-C_2S, Ge, CA_6
2	CaO, Lc	1250 1250	16 24	Kls, β-C_2S
3	C_2S, Lc	1250 1250	16 24	Ra, Kls
4	Ra, Lc	1250 1250	16 24	Kls, Wo
5	Ge, Lc, Mu	1250 1250	16 24	Ge, Lc
6	Ge, Mu, $KAlO_2$	1250 1250	23 64	Kls, CA_6, Ge
7	Kls, An, Wo	1250 1250	23 64	Lc, Ge, (An), Wo, Kls
10	$K_2Si_2O_5$, CA_6, SiO_2	1050 950	22 64	Melt, (unident. phase)
11	$K_2Si_2O_5$, CA_6, SiO_2	1050 950	22 64	Melt, (unident. phase)

$C_2S = Ca_2SiO_4$ Cor = Al_2O_3 Mu = $3Al_2O_3 \cdot 2SiO_2$

Lc = $KAlSi_2O_6$ Ksp = $KAlSi_3O_8$ An = $CaAl_2Si_2O_8$

$CA_6 = CaAl_{12}O_{19}$ Kls = $KAlSiO_4$ Wo = $CaSiO_3$

Ge = $Ca_2Al_2SiO_7$ Ra = $Ca_3Si_2O_7 = C_3S_2$ ( ) = phase barely detectable by x-ray diffraction

Reactions 1, 2, 3, 4, 6 and 7 have unquestionably gone to the right. The existence of extra phases among the products of reactions 1, 6 and 7 is probably a matter of incomplete reaction. In the case of reaction 5, the mullite peak detectable in the starting material disappears with concomitant increase in intensity of the leucite lines. This observation has been made in numerous other experiments, and all results taken together constitute very strong evidence for extension of a leucite (ss) field toward potassium-deficient compositions. However, the long-term equilibrations discussed above indicate that the Kls + An tie line is probably stable; therefore, the existence of Lc (ss) + Ge at the expense of Kls + An in tie line reaction 5 is possibly a kinetic phenomenon. Alternatively, there may be a Kls (ss) field such that Kls coexisting with An is potassium deficient. Hopefully, this problem will be resolved during the ensuing quarters.

3. Glass Crystallization Experiments

A third type of experiment designed to test phase relations proposed in Fig. 2 involves melting mixtures from the postulated four-phase volumes, quenching to a glass, crushing and crystallizing. Previously, this type of experiment was not successful owing to incomplete crystallization. The effect of periodic grinding and slight hydration will possibly prove beneficial in this respect. These experiments are not yet complete and results will be discussed in the next quarterly report.

Plans: Continue analysis of K data in an attempt to determine simple relationship relating K pressure to composition. Determine new data or verify existing data as required.

Finalize subsolidus equilibria in (Si, Al)-rich K_2O-CaO-Al_2O_3-SiO_2 and prepare results for formal publication. Determine accurately the composition of 13 minimum melts in the quarternary system. Continue efforts at modeling quarternary liquidus surfaces. Continue study of subsolidus equilibria in K_2O-rich portion of system involving K_2CaSiO_4 and $K_2Si_2O_5$.

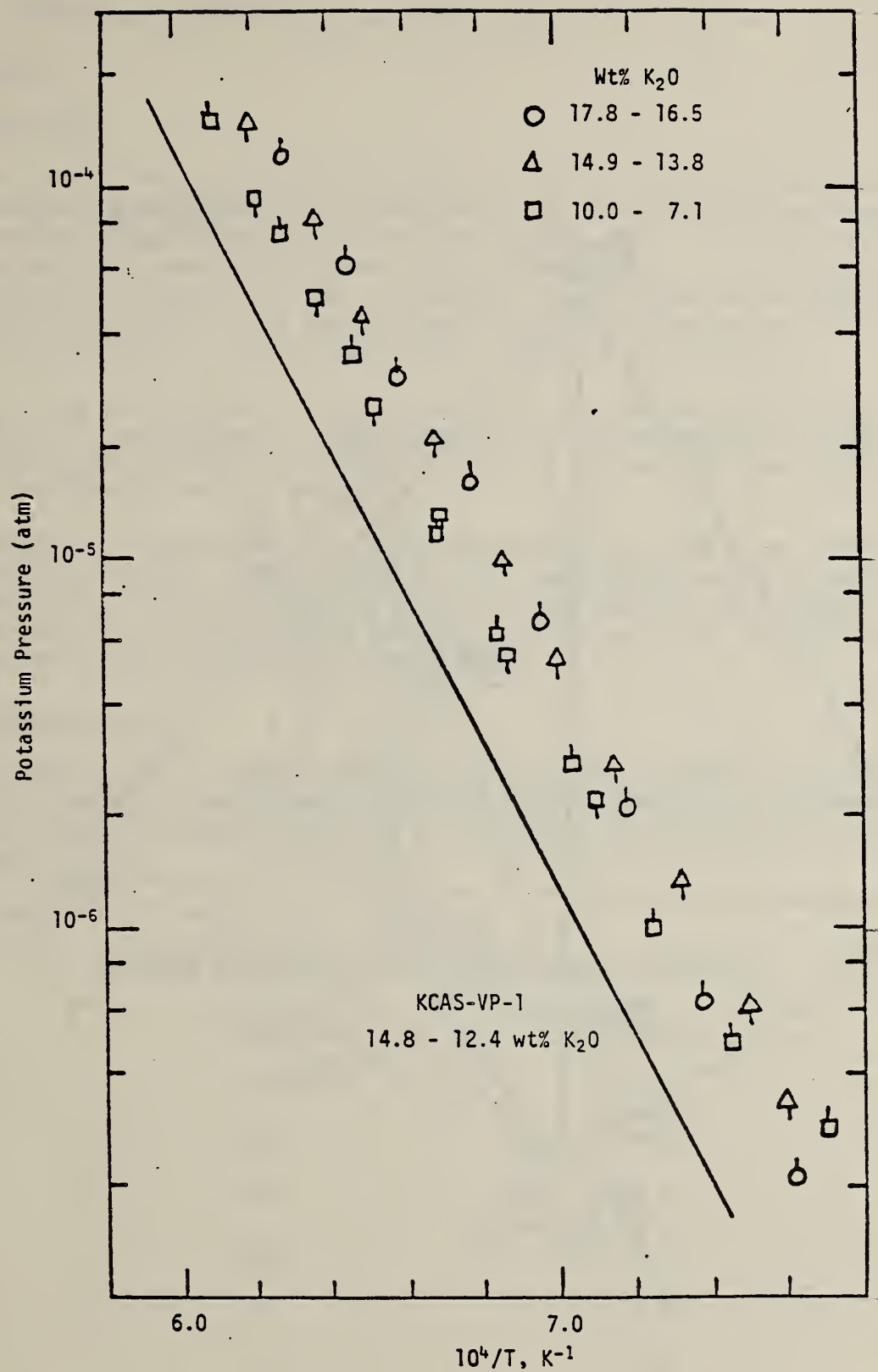

Figure 1. Selected vapor pressures of K above KCAS-VP-4 sample at noted bulk composition of K_2O vs $10^4/T$. The straight line represents the K pressure over KCAS-VP-1 sample in the K_2O bulk composition range 14.8-12.4 wt% K_2O. Upward or downward tics on points indicate whether temperatures were increased or decreased during the experimental sequence.

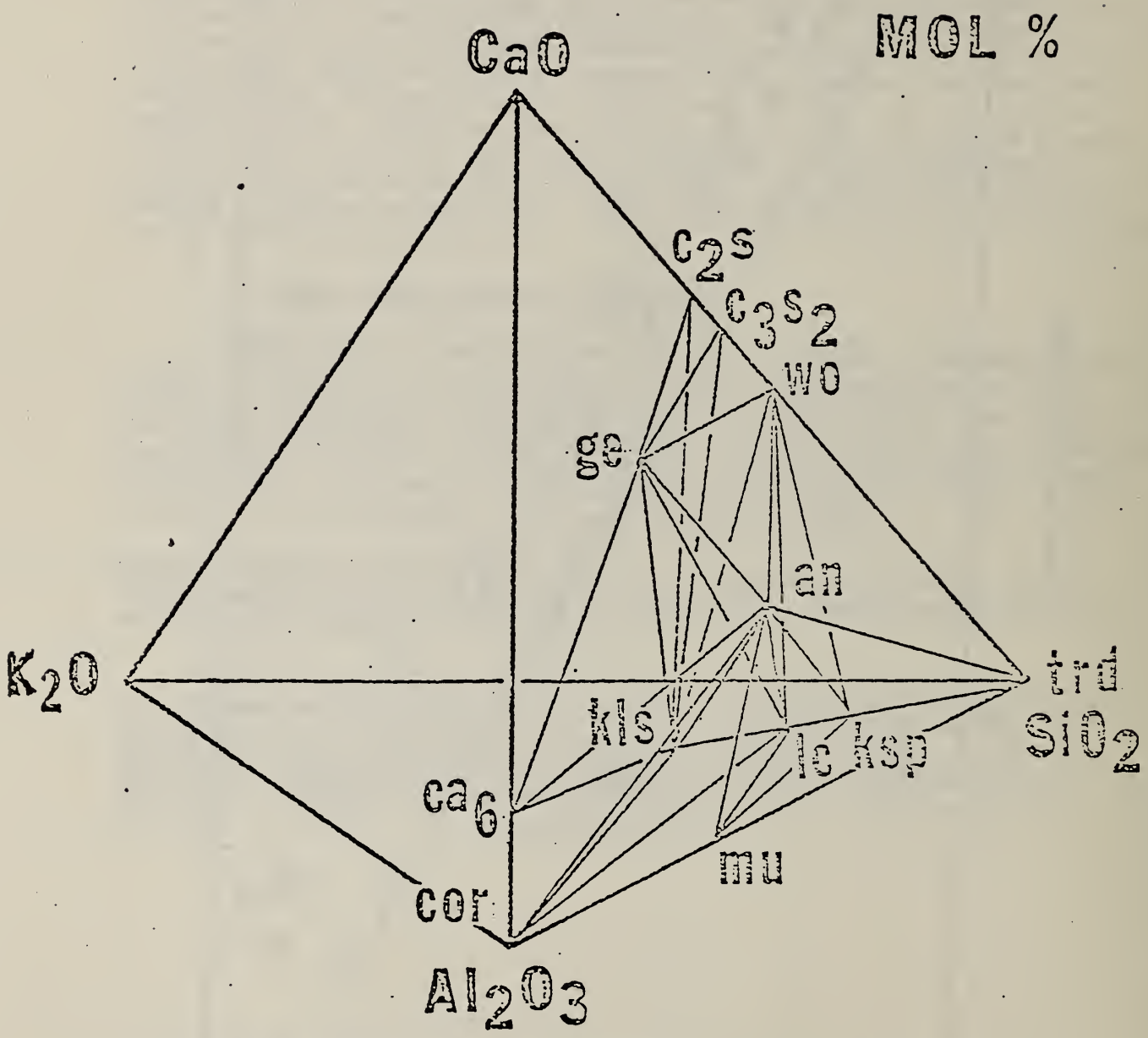

Figure 2. Subsolidus relations for synthetic $CaO-K_2O-Al_2O_3-SiO_2$ slags, as previously postulated in April-June (1978) Quarterly Report (refer to Table 3 for abbreviations).

2. Electrical Conductivity and Polarization (W. R. Hosler)

Progress:

Introduction

In the last quarterly report (July-Sept. 1980), four probe AC electrical conductivity measurements were compared with four probe DC measurements on slag from a coal burning steam plant in Bow, NH. AC and DC data agree quite well with some differences existing near 1100 °C. These measurements supported the suggestion made in previous reports that above 1385 °C, ionic conductivity is the predominant transport mechanism in this particular slag which contains a relatively large amount of iron (~14%).

During this quarter, work has continued on the investigation of the conductivity mechanisms in slag containing a lesser amount of iron (3-4%) than has been studied previously. This slag is derived from coal mined from the Rosebud seam in Montana.

A conductivity measurement has also been made on a sample of yttria stabilized zirconia. The purpose of this measurement was not necessarily to determine the conductivity of ZrO_2, but to test the measurement technique using the comparison between four probe AC and DC methods as discussed in the previous quarterly report.

Slag Conductivity

Four probe AC and DC measurements have been made on several samples of slag derived from coal from the Rosebud seam in Montana. An elemental analysis of this slag as received from Montana State University is given in Table 1.

Table I

Analysis of Rosebud slag (independent laboratory)

Element	w/o
Si	20.3
Fe	3.9
Al	10.9
Mg	3.8
Ca	13.3
K	0.3
Na	0.4

This slag is considerably lower in iron content than the Eastern slag measured previously, but has a larger amount of calcium. 20 w/o K_2SO_4 has been added to the base slag. In the process of adding the potassium, phase separation occurs and some of the potassium is rejected (see QR July-Sept. and October, 1973) so that the final material contains less potassium than is indicated by the amount of K_2SO_4 added. This potassium rejection is enhanced with slags containing large amounts of calcium. An analysis for final potassium will be obtained and the electrical properties over the temperature range from 500 to 1500 °C will be given in a later report. It became evident during initial measurements, that long times were required at certain temperatures to reach a state in the sample where the conductivity did not change with time at a given temperature. If one sets an arbitrary rate of change of conductivity below which the absolute conductivity magnitude change is negligible for a very long time, then it is possible to complete a set of measurements in some finite time (for example, one week) and approach closely an equilibrated value of conductivity. This approach is not valid, however, at low temperatures where initial conductivity changes with time are small when a new temperature point is established and thermal kinetics prevent an equilibrated process in a reasonable time. The dividing line in this material below which an equilibrated value ($\Delta\sigma/\Delta\tau$ < 50 ppm/hour) of conductivity cannot be obtained easily is near 1000 °C. Therefore, it seems prudent to discuss only the data above 1000 °C as characteristic of the material at a given temperature. Data at lower temperatures is dependent on the past treatment and cannot be treated as characteristic of the material without qualifications.

In the Seventh International Conference on MHD Electrical Power Generation held at MIT, Cambridge, Massachusetts, June 16-20, 1980, in session 07, the conductivity of Eastern slags is discussed. Two distinct slopes in the conductivity vs 1/T curves are shown for those slags (containing no added potassium) above 1100 °C. The conductivity of all Bow, NH slag samples containing iron in the amount as received (14 w/o) as well as those with added iron show a two slope region in this high temperature range. The slope at the highest temperatures gives an activation energy of approximately 1.8 eV while the steeper slope at lower temperatures varies giving an apparent activation energy up to near 4.0 eV. The slope in the lower temperature region is very sensitive to the equilibration time allowed. In earlier measurements, careful enough attention was not paid to this time effect. In the Rosebud slag, the high temperature slope again appears to be the same as that for the Eastern slag but the magnitude of the conductivity in that temperature range is reduced by approximately a factor of three. The slope at the highest temperatures is shown in Figure 1 for slags with different iron content and for Eastern and Western slags which have different base compositions. It demonstrates that the conductivity in this region is some type of activated process with an activation energy independent of the iron content, but that the magnitude of the conductivity is dependent on the iron content.

In the QR July-Sept. 1972 from this laboratory, there was a discussion of the conduction mechanism in slag samples particularly with respect to the iron content and the semiconducting electron exchange between the Fe^{+2} and the Fe^{+3} ions. The activation energies displayed by the high temperature data in these slag samples is higher than would be expected from a semiconducting transition involving the iron. Since σ (conductivity) = $ne\mu$ where n is the concentration of the current transport carrier which remains nearly constant with T, and μ is the mobility of that carrier, the mobility may be the predominant activated process which itself would then depend on the phase composition of the material in a given temperature range. The phase composition of these slags must be studied in correlation with the temperature ranges where the data shows these activated processes. This can be done by equilibrating a sample at a given temperature within the range of interest and quenching to room temperature with subsequent analyses by SEM and XRD techniques. Careful attention must be paid also to the viscosity of the slag above the melting point and its possible effect on the conductivity.

ZrO_2 Conductivity

The material used for this experiment was cut from a ZrO_2 tube of very high density which was used as an oxygen sensor. In order to test the four probe AC-DC comparison method of measurement, it is desirable to have a completely ionic conductor and to have the contacting electrodes completely irreversible to the ionic species conducting. It is well known that ZrO_2 is an oxygen ion conductor which makes it useful as an oxygen sensor material. In a sensor, however, the contacting electrodes must be reversible to oxygen. Contacts are usually porous platinum. In the case for these measurements, platinum was also used but the leads were attached in the same manner as described in the quarterly report (April-June 1980) and platinum in these contacts does not appear to be porous. Figure 2 shows a plot of the DC and the AC (40Hz) conductivity measured in air. The curves are identical as expected and furthermore, the conductivity versus frequency (40Hz to 40KHz) plots show no conductivity change with frequency. Similar measurements were made in an atmosphere of 1.2×10^{-5} ppm O_2 in N_2 and the bulk conductivity did not change. For those measurements carried out in an air atmosphere, there is little difference between the voltage values measured on the current carrying probes i.e., V_{12} and V_{34} (see previous quarterly report) with respect to AC and DC measurements. This indicates that no oxygen ion buildup or depletion is evident at the electrodes and exchange takes place rapidly contrary to what was expected. For those measurements done at the low oxygen pressure, the DC measurements did show some slight polarization (increase in V_{12} and V_{34}) compared to the AC data on the same probes at 40Hz. When the sample was removed from the holder and examined, a darkened area located symmetrically around the current probes (probes 1 and 4) was evident. Apparently in a reduced oxygen pressure reduction of the oxide to zirconium can occur rapidly at the cathode when an electric field (1-2 v/cm) is applied, particularly at elevated temperatures (above

1200 °C). At the same time, reoxidation should take place at the anode. During the DC portion of the measurement, current was left on the sample for approximately 60 seconds during each data acquisition at each temperature point and reversed for the same length of time so no net reduction should show at a particular current probe. The net reduction observed must be due to the lack of oxygen available in the atmosphere for reoxidation when a current carrying probe becomes an anode. Therefore, oxidation is a less rapid process than reduction in ZrO_2 under an ambient partial pressure of oxygen of near one part per million. This causes a polarization effect near the current contacts as the data shows in Figure 3 for the DC measurement. No such effect was observed for those measurements in air. This material, it turns out, was not well suited to demonstrate the viability of the analytical technique used in slag conductivity measurements because electrode reversibility with the respect to the transported ion (oxygen) is not zero and the ion is also a component in the atmosphere so that exchange can take place in near-electrode areas, thus eliminating polarization (in an air atmosphere). Another known ionically conducting material should be used where the conducting ion does not react with the electrode material and does not readily exchange with the ambient atmosphere up to approximately 1500 °C.

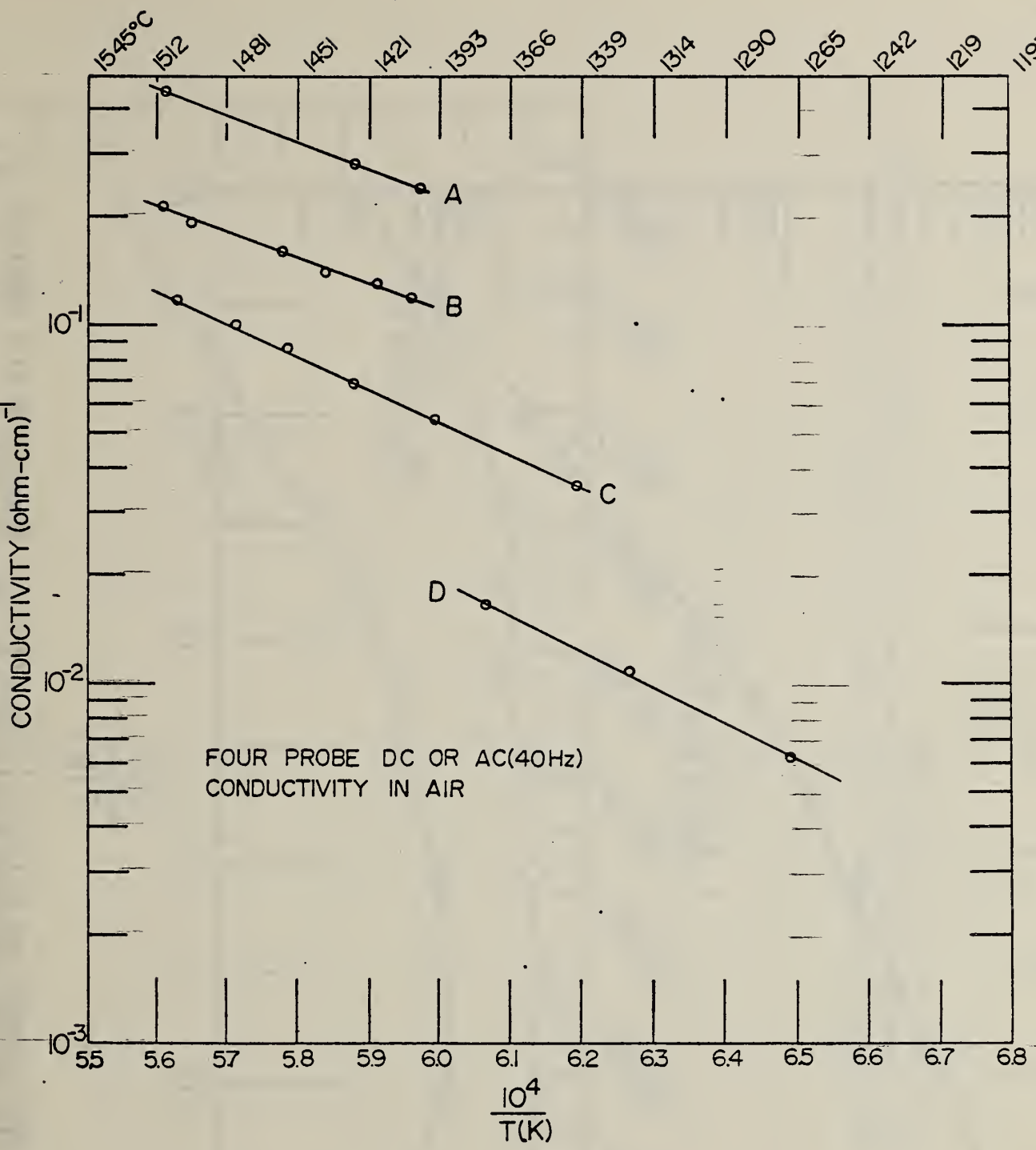

Figure 1. Electrical conductivity vs. temperature of several slags containing amounts of iron. A, B, and C are Eastern slags (Bow, NH) containing 29, 20, and 14 weight percent Fe respectively, but with no added potassium. (See QR April - June 1979, page 33, for base composition). D is a Western slag (Rosebud seam) with 4% iron and with 20% K_2SO_4 added to the melt. (See Table 1, this report, for base composition).

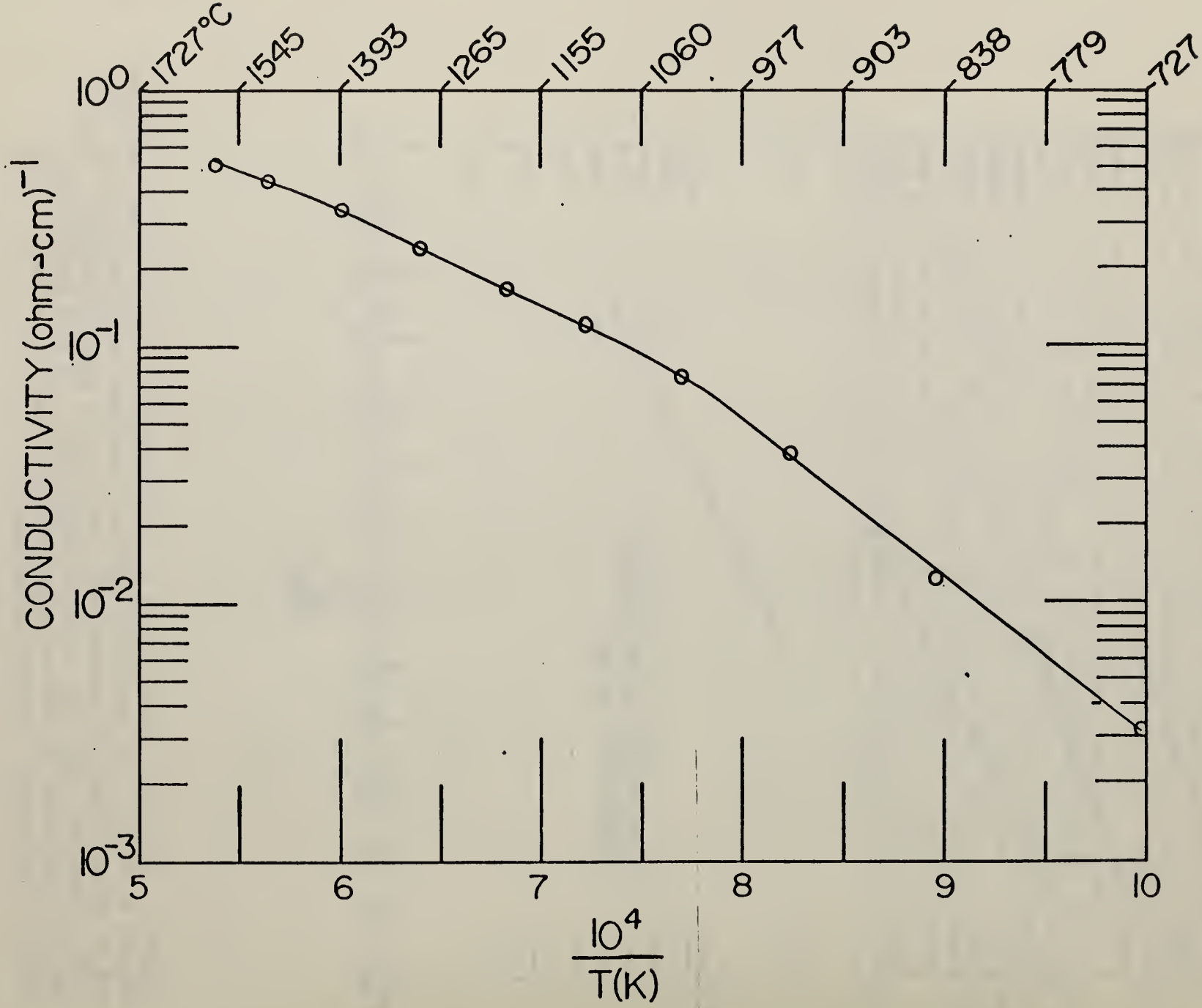

Figure 2. Four probe DC and AC (40 Hz) conductivity vs. temperature of a sample of high density yttria stabilized zirconia measured in air.

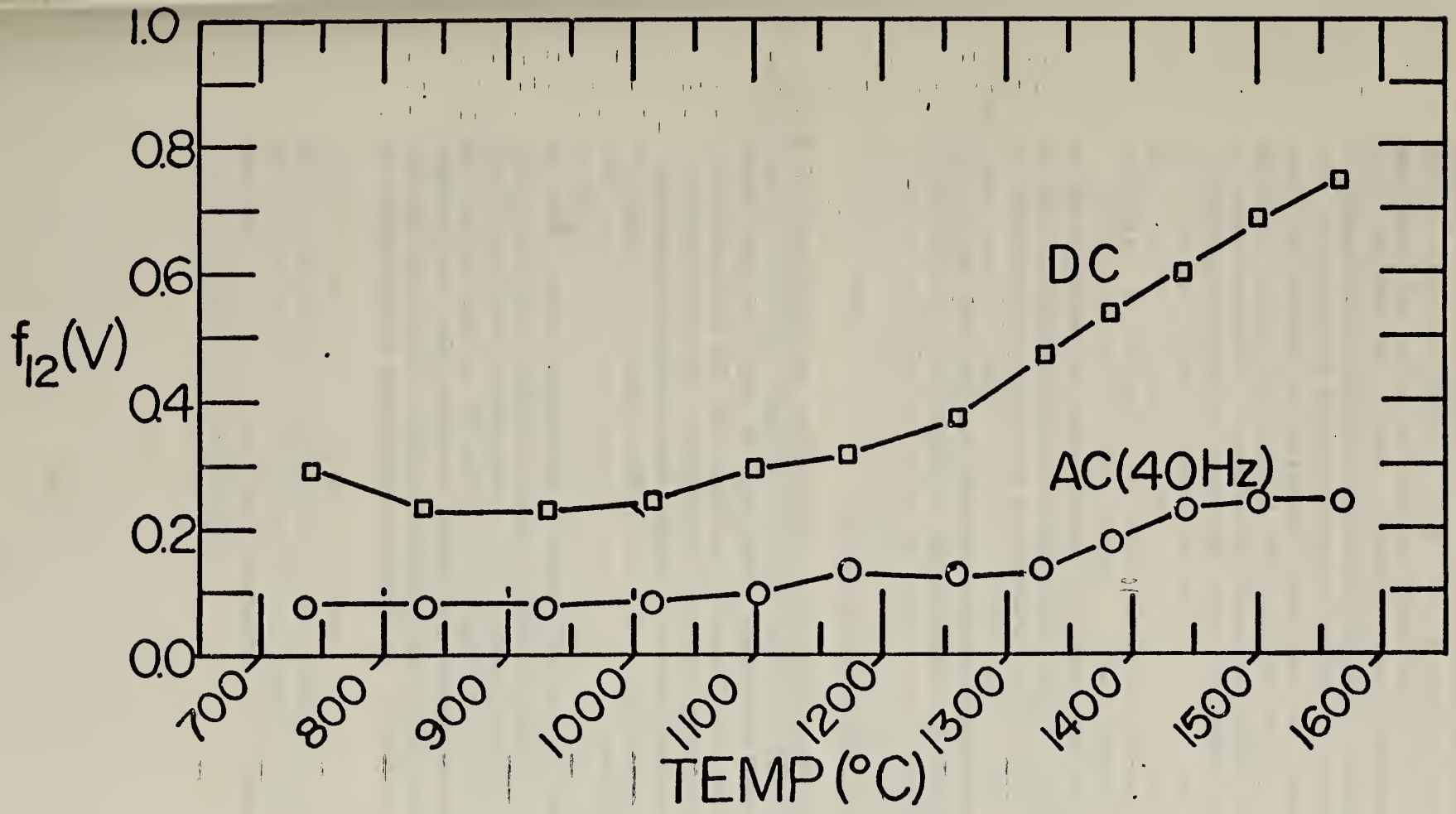

Figure 3. Plot showing the effect of polarization on the current carrying electrodes in yttria stabilized zirconia when an electric field is applied in an atmosphere of 1.2 ppm O_2 in N_2. $f_{12}(V)$ equals

$$\frac{\frac{V_{12}}{d_{12}}}{V_{23}\cdot\frac{1}{d_{23}}} - 1$$

where V_{12} and V_{23} are the voltages measured between probes 1 and 2 and between probes 2 and 3 respectively. d_{12} and d_{23} are the distances between these probes. (See text and previous quarterly report for a description of the measurement.)

3. Corrosion of Downstream MHD Components (J. Smit and C. D. Olson)

Progress: Tests were continued on 316 stainless steel for suitability as a downstream MHD component material.

Two samples of 316 stainless steel were exposed to corrosive gas stream environments, at wall temperatures of 500 °C. Sample 7-6 (Figure 1) was maintained in an oxygen rich gas stream environment while sample 10-6 (Figure 2) was exposed to a fuel rich gas stream environment. The gas stream environment, as previously reported, is determined by varying the oxygen-propane gas ratio. Both tubular specimens, 12.5 mm in diameter, 250 mm in length, and with 0.8 mm wall thickness were exposed for a four hour period of time, exclusive of heat-up and cool down time.

The hot gas stream was seeded with a mixture of 20 percent by weight K_2SO_4 and 80 percent by weight K_2CO_3. Seeding of the hot gas stream occurred during the first 25 minutes of the test run at the rate of 10 grams per minute. The gas stream temperature was maintained at 1300 °C and monitored with a Pt/Pt-10%Rh thermocouple placed in close proximity to the center of the sample tubes, while the wall temperature was monitored using a Pt/Pt-10%Rh thermocouple welded into the wall of the tube at the midpoint position. Cooling air was used to maintain the tube wall temperature of the samples.

SEM/EDX Analysis of the Metal-Salt Interface

After the four hour test run the samples were cooled to approximately 40 °C and immediately encapsulated in epoxy resin to prevent possible contamination and hydration to the sample coatings. Sections for analysis were taken 10 mm from the midpoint of the tube and prepared for SEM/EDX analysis. The sections were ground and polished using standard metallographic techniques. Specimen preparation was accomplished using a non-aqueous medium and specimens were stored in a vacuum dessicator to minimize hydration and contamination.

Both specimens exhibited similar salt deposit characteristics. The surface facing the gas stream was thinner than the deposit on the side portion of the tube (drip zone), and a thin fume deposit was found on the underside of the tube. The thickness of the top surface deposit was found to be consistent with previous samples, in that, the surface salt deposit is thinner as the wall temperature increases. Also that under fuel rich conditions the deposit is thinner than in the oxygen rich environment.

Examination and comparisons can be made with 7-6 and 10-6. Both samples were seeded with 80 percent by weight K_2CO_3 and 20 percent by weight K_2SO_4, with wall temperature of 500 °C, however 7-6 was in an oxygen rich environment and 10-6 was in a fuel rich environment. As seen in previous samples (8-6, 9-6) a banding can be observed in the coating (Figure 3) showing a region of K + S near the surface of the steel followed by a high K region with a thin band of K + S on the surface of the coating. However, the bulk of the coating is generally high in potassium (K) with moderate amounts of sulfur (S) found. The corrosion process exhibited in both specimens seem to follow the same general corrosion mechanism as found previously. The cations are found in a general order of mobility where: a) bulk stainless steel, b) higher nickel-high chromium-iron, c) chromium-iron-nickel-potassium, d) chromium-higher iron-potassium, e) iron-potassium, f) high potassium. Again sulfur is found in small quantities in the reaction zone area and coating.

At the lower wall temperature of 500 °C, the corrosion process is not as vivid as samples examined at 590 °C (8-6, 9-6) however, the process was observed and noted to be similar in nature as described above.

Conclusion: As stated previously the variance between fuel rich and oxygen rich environments in the presence of K_2CO_3 and K_2SO_4 are minimal. Corrosion of type 316 stainless steel seems to occur readily in both instances. In general, therefore, both systems indicate the same metal cation movement from the bulk stainless steel into the salt deposit.

Clad Materials for Application in Downstream MHD Components

Recently much interest has been generated in regard to the suitability of clad materials for application in downstream MHD components. This interest stems not only from a standpoint of corrosion reduction (durability) but also from a standpoint of economics (reduction of consumption of scarce resources). Attention therefore is now being given to a class of materials that are arc plasma sprayed on metals. Three commercially available examples of arc plasma sprayed materials are presently under consideration for testing and evaluation. These coatings, NiCrAlY, $MgAl_2O_4$ (spinel), and ZrO_2 (doped with MgO) have been sprayed on a mild steel tube AISI 1015) substrate. The coating thickness averages 0.5 mm. Short length specimens of each, 75 mm in length and 0.9 mm wall thickness, have been obtained for temperature cycling, and thermal shock tests. Longer specimens, 0.25 m, have been obtained with Pt/Pt-10%Rh thermocouples embedded at the midpoint for corrosion testing.

SEM/EDX examination of these specimens prior to testing is currently being undertaken. Evaluation of the boundaries between substrate (steel) and the cermet are of importance for adhesion properties. Surface examination will reveal areas susceptible to penetration of possible corrosive materials (porosity).

SEM/EDX evaluation will also include heat treated specimens. These samples have been cycled from 18 °C ↔ 700 °C in air and another set of identical samples have been cycled from 18 °C ↔ 700 °C in forming gas (5% H_2, 95% N_2). Analysis of these sets should reveal any tendency toward delamination or deformity in the cermet bonded material.

Plans: (1) Continuation of SEM/EDX analysis of the arc plasma sprayed coatings, to include specimens exposed to seeded hot gas stream, (2) to initiate exposure studies on 2 1/4 - 1 Mo. Croloy tubing.

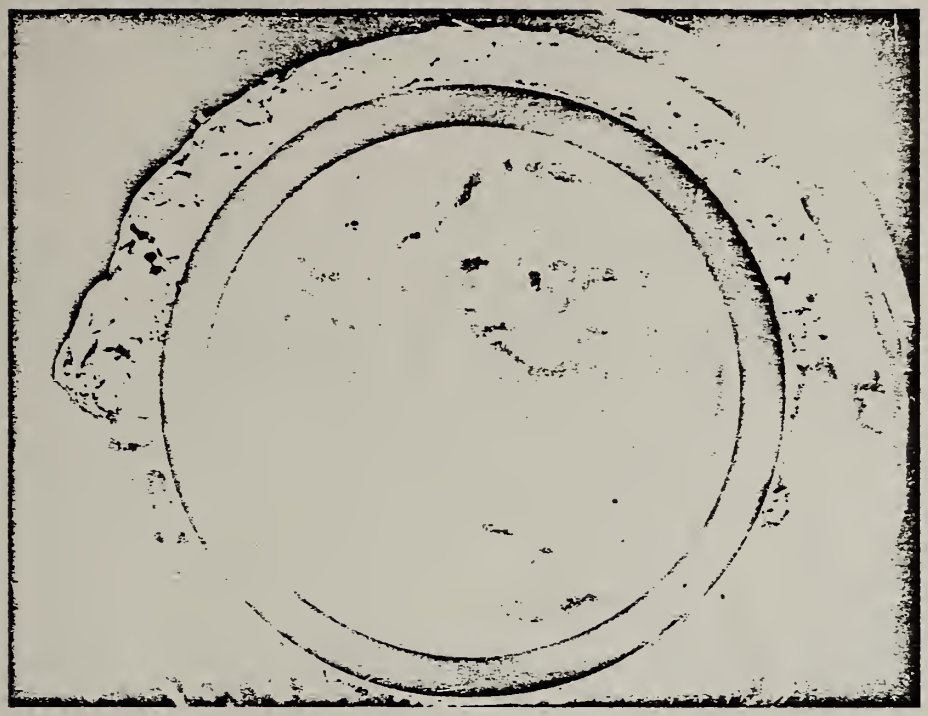

Fig. 1 Section of Type 316 stainless steel tubing after exposure to K_2CO_3/K_2SO_4 seeded oxygen rich hot gas stream. Tube wall temperature 500°C. 6x.

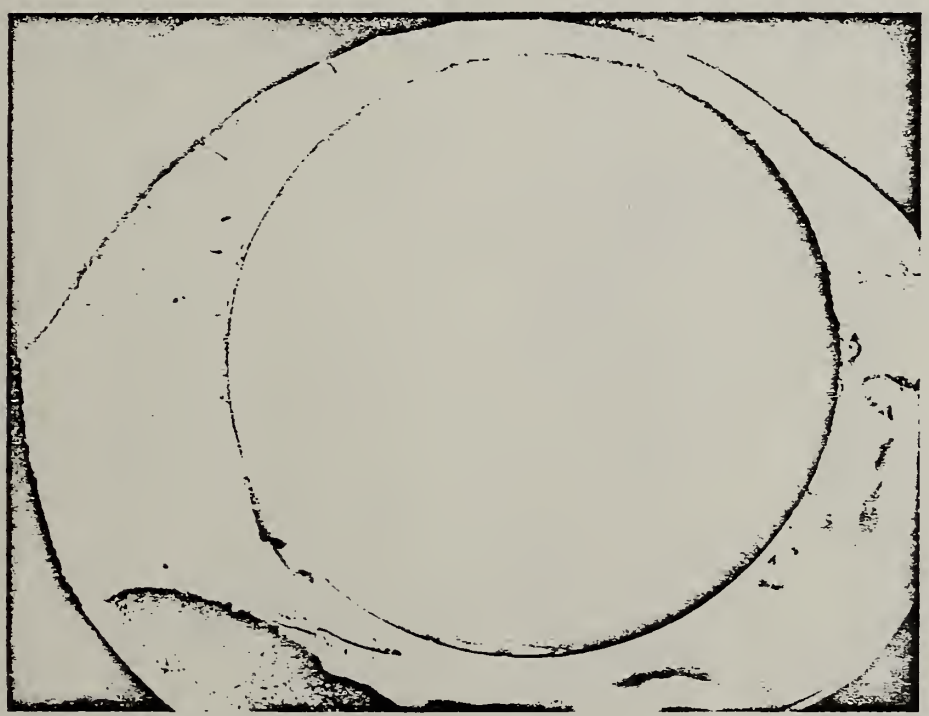

Fig. 2 Section of Type 316 stainless steel tubing after exposure to K_2CO_3/K_2SO_4 seeded fuel rich hot gas stream. Tube wall temperature 500°C. 6x.

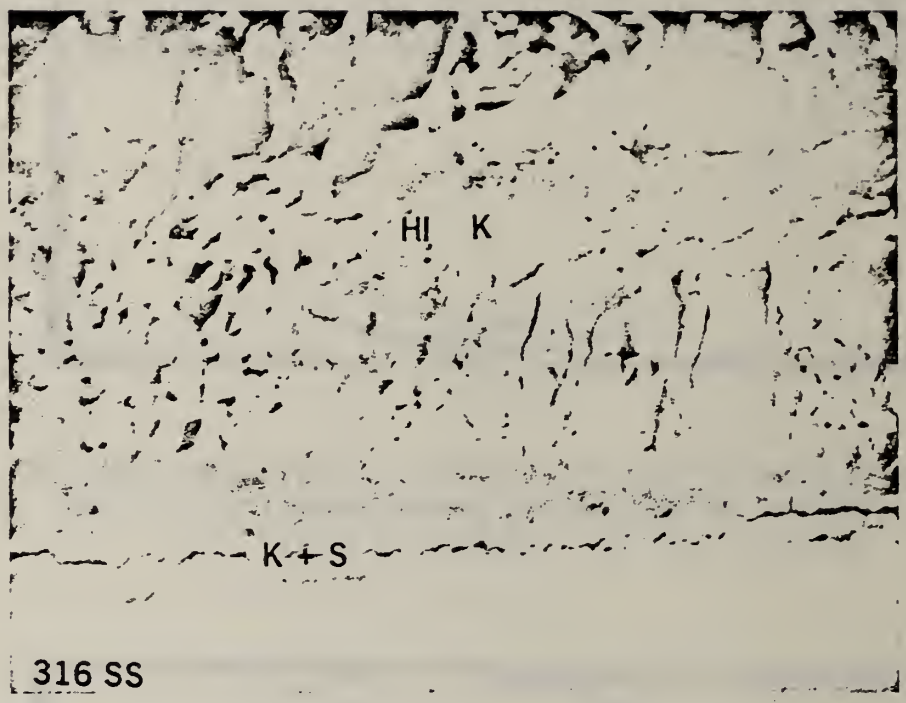

Fig. 3 SEM micrograph, 425 x, of stainless steel-salt deposit reaction zone of specimen shown in figure 1.